

Supplementary Material: Identifiability of Differential-Algebraic Systems

Arthur N. Montanari^a, François Lamoline^b, Robert Berezina^c, Jorge Gonçalves^{b,d}

^aDepartment of Physics and Astronomy, Northwestern University, Evanston, IL 60208, USA

^bLuxembourg Centre for Systems Biomedicine, University of Luxembourg, Belvaux L-4367, Luxembourg

^cDivision of Decision and Control Systems, KTH Royal Institute of Technology, Stockholm SE-100 44, Sweden

^dDepartment of Plant Sciences, Cambridge University, Cambridge CB2 3EA, United Kingdom

S1 Identifiability analysis of chemical reactor

Consider an exothermic reactor system with a single first-order reaction ($A \xrightarrow{r(t)} B$) and generated heat removed through an external cooling circuit. The chemical reactor is modeled by [1]

$$\dot{x}_1 = k_1(c_0 - x_1) - x_3 \quad (\text{S1a})$$

$$\dot{x}_2 = k_1(T_0 - x_2) + k_2x_3 + k_3(T_c - x_2), \quad (\text{S1b})$$

$$0 = x_3 - k_5 \exp\{-k_4/x_2\}x_1, \quad (\text{S1c})$$

where $\mathbf{x} = [x_1 \ x_2 \ x_3]^\top \in \mathbb{R}^3$ is the state vector, x_1 is the concentration of reactant A, x_2 is the temperature, and x_3 is the reaction rate per unit volume (algebraic variable). Eq. (S1c) arises from a conservation law¹ (Arrhenius equation) that imposes the dependence of reaction rates on temperature. The parameters are: inlet feed reactant concentration c_0 and feed temperature T_0 , coolant temperature T_c , and other constants k_i . Fig. S2 shows that the chemical reactor dynamics converge to a limit cycle for the considered set of parameters.

Let the coolant temperature be the parameter sought to be identified (i.e., $\theta = T_c$). The accuracy of parameter estimation depends on the choice of observable, that is, which state variable x_i is measured by a sensor. To determine the most suitable sensor data for parameter estimation, we now test which observables ensure parameter identifiability. As a tutorial, we analyze the identifiability of the descriptor model (S1) step-by-step, considering the output signal $y(t) = x_1(t)$, $t \in [0, 10]$ s. First, we augment model (S1) by representing $\theta(t) = T_c(t)$ as an additional state variable with constant dynamics, i.e., $\dot{\theta}(t) = 0$. Functions $\bar{\mathbf{H}}_\nu$ and $\bar{\mathbf{F}}_\mu$ are then constructed up to order $\mu = \nu = n - 1 = 2$. Thus, $\bar{\mathbf{H}}_\nu = [x_1 \ \dot{x}_1 \ \ddot{x}_1]^\top$ and $\bar{\mathbf{F}}_\mu = [(\mathbf{F})^\top \ (\frac{d\mathbf{F}}{dt})^\top \ (\frac{d^2\mathbf{F}}{dt^2})^\top]^\top$, where

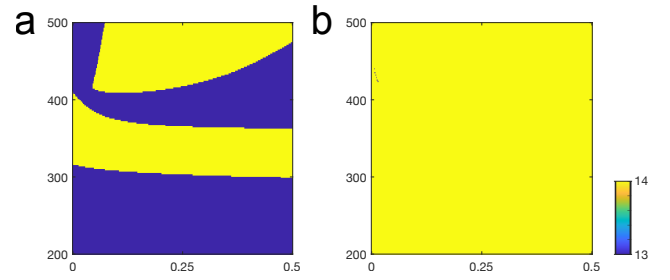


Fig. S1. Numerical values corresponding to (a) the left-hand side (LHS) and (b) the right-hand side (RHS) of Eq. (12) locally evaluated at each state \mathbf{x} in the phase plane (x_1, x_2) . The tolerance for the numerical rank computation is set to $\max_{\mathbf{x}} \sigma n \epsilon (\|\mathcal{I}(\theta, \mathbf{z})\|_2) = 10^{-6}$, where $\epsilon(\cdot)$ indicates the floating-point relative accuracy of a number. This tolerance ensures that the rank analysis is consistent for all states $(x_1, x_2) \in [0, 0.5] \times [200, 500]$.

$$\mathbf{F} = \begin{bmatrix} k_1(c_0 - x_1) - x_3 - \dot{x}_1 \\ k_1(T_0 - x_2) + k_2x_3 + k_3(\theta - x_2) - \dot{x}_2 \\ x_3 - k_5 \exp\left\{-\frac{k_4}{x_2}\right\}x_1 \\ \dot{\theta} \end{bmatrix},$$

$$\frac{d\mathbf{F}}{dt} = \begin{bmatrix} -k_1\dot{x}_1 - \dot{x}_3 - \ddot{x}_1 \\ -k_1\dot{x}_2 + k_2\dot{x}_3 + k_3(\dot{\theta} - \dot{x}_2) - \ddot{x}_2 \\ -\dot{x}_3 - k_5 \exp\left\{-\frac{k_4}{x_2}\right\} \left(\dot{x}_1 + k_4 \frac{x_1 \dot{x}_2}{x_2^2}\right) \\ 0 \end{bmatrix},$$

and $d^2\mathbf{F}/dt^2$ is omitted for the sake of brevity. Note that $\bar{\mathbf{F}}_\mu$ and $\bar{\mathbf{H}}_\nu$ are functions of θ , \mathbf{x} , and its time derivatives. By assumption, $\dot{\theta} = \ddot{\theta} = \ddot{\theta} = 0$, $\forall t$. After building the identifiability matrix (11), condition (12) can then be locally evaluated to test if the system is identifiable at any consistent state $\mathbf{x}_0 \in \mathbb{L} \subset \mathbb{R}^3$ and parameter value $\theta_0 \in \mathbb{R}^1$. Fig. S1a shows the rank of the identifiability

¹ This descriptor model can be directly converted to ODEs and then numerically integrated with conventional solvers (e.g., 4th-order Runge-Kutta). However, numerical solvers for DAEs enforce the constraint (S1c) to be preserved in simulations as in Fig. S2.

bility matrix $\mathcal{I}(\boldsymbol{\theta}, \mathbf{z})$ for every state \mathbf{x} in the phase plane (x_1, x_2) . Local identifiability of $\boldsymbol{\theta}$ is guaranteed for states in which the values computed for the LHS (Fig. S1a) and RHS (Fig. S1b) of Eq. (12) are equal.

Fig. S2 shows the identifiable and unidentifiable regions in the state space depending on the observable choice. For the output $y(t) = x_1(t)$ (Fig. S2a), the limit cycle solution $\Phi(\mathbf{x}(0); \theta)$ predominantly lies in an unidentifiable region. Following Definition 4, at an unidentifiable state \mathbf{x}_0 , measured trajectories $\mathbf{h} \circ \Phi(\mathbf{x}_0; \theta)$ sufficiently close to \mathbf{x}_0 are *not* guaranteed to be distinguishable from a trajectory $\mathbf{h} \circ \Phi(\mathbf{x}_0; \theta')$ corresponding to some distinct parameter $\theta' \neq \theta$ lying in a neighborhood \mathcal{U} of the true parameter value θ . In other words, there may exist some $(\theta' \in \mathcal{U}) \neq \theta$ such that $\mathbf{h} \circ \Phi(\mathbf{x}_0; \theta) = \mathbf{h} \circ \Phi(\mathbf{x}_0; \theta')$. The predominance of unidentifiable regions in the state space implies the possible existence of non-unique solutions for θ in the neighborhood of $\Phi(\mathbf{x}(0); \theta)$. As a result, if the dataset primarily comprises measurement data collected from these unidentifiable states, the estimation accuracy of θ may be compromised.

Despite the predominance of unidentifiable regions in Fig. S2a, parameter identifiability is achieved in a small region of the limit cycle around $\mathbf{x} = [0.25 \ 360 \ 0.5]^T$ (as well as other regions containing part of the transient response). Theoretically, parameter estimation could be possible by using data collected solely at these identifiable states. However, this may not be possible in practice if the identifiable region is too small (as in Fig. S2a) due to limited data availability. Moreover, we note that such analysis depends on the choice of tolerances for the rank computation, as presented in Fig. S1. Regions of identifiable/unidentifiable states may expand or shrink depending on the tolerance value. If the rank tolerances are not appropriately chosen, condition (12) may be numerically satisfied for ill-conditioned matrices $\mathcal{I}(\boldsymbol{\theta}, \mathbf{z})$, even when the system is practically unidentifiable.

After conducting the same identifiability analysis for $y(t) = x_2(t)$ and $y(t) = x_3(t)$, Fig. S2b,c shows that the system is locally identifiable everywhere around the limit cycle solution when these other types of measurement signals (sensors) are considered. This is a particularly beneficial result for this sensor placement problem since temperature sensors ($y = x_2$) are very affordable and practical to install in chemical reactors.

References

- [1] W. H. Ray, Advanced Process Control, New York: McGraw-Hill, 1981.

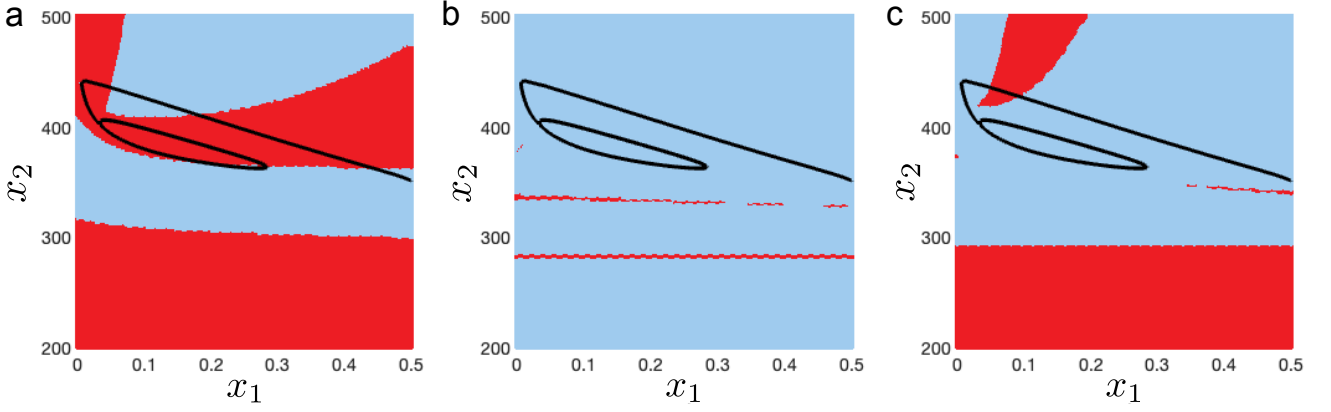


Fig. S2. Identifiable regions of the chemical reactor model for measurement signals given by: **(a)** $y = x_1$, **(b)** $y = x_2$, and **(c)** $y = x_3$. The blue (red) colors correspond to states \mathbf{x} in which the parameter T_c is identifiable (unidentifiable). The black solid line represents the state trajectory $\mathbf{x}(t)$ starting at the initial condition $\mathbf{x}(0) = [0.5 \ 350 \ 0.4995]^\top$ and converging to a limit cycle. The system parameters were set to $(c_0, T_0, T_c) = (1, 350, 305)$, and $(k_1, k_2, k_3, k_4, k_5) = (1, 209.205, 2.0921, 8.7503 \cdot 10^3, 7.2 \cdot 10^{10})$. The numerical simulations are shown using the `ode15s` solver in MATLAB.